JOURNAL OF MOLECULAR SPECTROSCOPY 146, 375–380 (1991)

Pressure Broadening of the 118.455 cm^{-1} Rotational Lines of OH by H_2, He, N_2, and O_2

K. V. CHANCE

Harvard-Smithsonian Center for Astrophysics

D. A. JENNINGS AND K. M. EVENSON

National Institute for Standards and Technology

M. D. VANEK, I. G. NOLT, AND J. V. RADOSTITZ

NASA Langley Research Center

AND

K. PARK

Department of Physics, University of Oregon

We have measured pressure broadening of the 118.455 cm^{-1} (3.551 THz) F_1, $7/2^+ \leftarrow F_1$, $5/2^-$ rotational lines of OH by H_2, He, N_2, and O_2. The measurements were made using tunable far-infrared spectroscopy. Broadening coefficients for N_2 and O_2 are presented for the temperature range 296 to 210 K; H_2 and He broadening coefficients are presented for the temperature range of 296 to 80 K. We also determined accurate values for the line positions. The line positions and their 2σ uncertainties are 3 551 185.36(4) MHz ($F = 4 \leftarrow 3$) and 3 551 204.42(4) MHz ($F = 3 \leftarrow 2$).

INTRODUCTION

The OH radical has a primary role in stratospheric photochemistry due to its involvement in odd oxygen loss through the HO_x catalytic cycle and to its involvement in reactions coupled to the chemistry of the halogen and nitrogen families. Measurement of stratospheric OH is thus a priority in current upper atmospheric research. The far-infrared rotational lines of OH can be readily measured in the middle and upper stratosphere from thermal emission, because the lines are quite strong and relatively free from interfering species. This type of measurement has the advantage of being able to measure OH through the diurnal cycle (*1*). Several techniques for measuring far-infrared emission from stratospheric OH have now been developed, including the use of Fourier transform spectrometers (*1–5*) and a Fabry–Perot instrument (H. M. Pickett, private communication, 1990). For the analysis of atmospheric spectra it is necessary to have accurate values of the molecular parameters of OH.

0022-2852/91 $3.00

Line positions and strengths for the far-infrared transitions have been determined very accurately (*6–9*). The OH lines are strong enough that line saturation must be properly accounted for in spectrum fitting and altitude profile retrieval. In order to do this, knowledge of the pressure broadening of the lines by air, including temperature dependence, is needed. This is the primary purpose of the present studies. The F_1, $7/2^+ \leftarrow F_1$, $5/2^-$ lines at 3.551 THz were chosen for our first comprehensive studies since they have been measured in the atmosphere by several groups (*1, 4, 5*) and since they are readily accessible for study using the techniques of far-infrared spectroscopy.

The rotational spectrum of OH is also of considerable current interest in astrophysics, where the far-infrared emission lines, including the lines in the present study, are measured in order to probe interstellar cloud conditions (*10–12*). Interpretation of the OH line measurements in terms of interstellar cloud physics requires a detailed knowledge of state-dependent cross sections for rotational excitation of OH by H_2 and, to a much lesser extent, by He (*13–15*). Pressure broadening of these lines is not ideal for providing information on collisional excitation, since broadening at collisional energies comparable to the transition energies involves both inelastic and elastic collisions, and since the interactions with individual states of the broadening gas are mixed. However, the pressure broadening coefficients still provide a useful check on the potential energy surfaces that are computed to calculate rotational excitation. Measurements of the pressure broadening of the OH lines by H_2 and by He are necessary in the present study in any case, in order to correct the O_2 and N_2 measurements for the H_2 and He required in the source chemistry of OH. The H_2 and He broadening measurements were extended to lower temperature (80 K) to provide further information on the intermolecular potentials for a range of interstellar cloud temperatures.

EXPERIMENTAL DETAILS

Tunable far-infrared radiation of high spectral purity was generated by the TuFIR method of CO_2 laser difference frequency generation with a metal–insulator–metal (MIM) diode (*16, 17*). Briefly, the radiation from two CO_2 lasers is combined on a beam splitter and focused onto the MIM diode, where the far-infrared difference is generated. One of the lasers is frequency modulated with a piezoelectric transducer and is frequency-locked to saturated fluorescence from a low-pressure CO_2 cell. The second laser is a cavity-tuned CO_2 waveguide laser that is frequency-offset locked to another stabilized CO_2 laser. The cavity tuning of the waveguide laser provides the sweep range (145 MHz) that is used in the present experiments. The far-infrared radiation generated by the MIM diode is frequency-modulated at the frequency of the modulated CO_2 laser. The absorption signal is detected as the modulation-broadened first derivative of the spectrum. The far-infrared frequency is known with an accuracy of ± 35 kHz and has a spectral purity of ~ 10 kHz. A length-scrambling device is used in these measurements to reduce standing waves in the far-infrared power spectrum. The Doppler widths of the OH transitions are 4.4 to 5.3 MHz (HWHM) for the temperature range of these studies. Thus, we can make fully resolved absorption measurements of the lineshape in order to determine the pressure broadening. This is necessary for studies of unstable molecules such as OH where the precise concentration of absorber is difficult both to determine and to maintain constant, making the curve-of-growth method for pressure broadening measurements impractical.

The absorption cell used in these studies is a 50-cm-long, 2.5-cm-diameter Pyrex tube equipped with double sets of high-density polyethylene windows. The cell was immersed in a temperature bath with the outer windows extending from either end. The inner windows are located several centimeters inside of the temperature bath, in order to maintain the OH and broadening gas at the bath temperature. The cell walls were coated with halocarbon wax to reduce wall loss of OH.

The overall cell pressure was monitored with a precision capacitance manometer, which sampled the pressure at the center of the cell length in order to minimize error due to pressure drop in the flow system (estimated at <1% in the worst case). Flow rates for H_2, He, N_2, and O_2 were monitored with precision flowmeter-controllers.

The bath was controlled at temperatures below ambient using slushes of ethylene glycol and chloroform and, for the lowest temperature, by filling with liquid nitrogen. The resultant temperatures for the OH absorption measurements were 296 ± 2, 259 ± 4, 210 ± 3, and 80 ± 3 K.

OH is produced from the reaction of hydrogen atoms, generated in a dc discharge, with NO_2 or with O_2. OH production and mixing with the broadening gas take place in a sidearm external to the absorption cell. The OH and broadening gas are pumped through a portion of the sidearm which is at the bath temperature to allow them to equilibrate to the cell temperature before broadening is measured. For these experiments, it was necessary to mix He with the H_2 in the discharge to produce sufficient OH at pressures higher than about 400 Pa. Therefore, He pressure broadening, as well as H_2 pressure broadening, was measured separately in order to correct the results for broadening by gas mixtures.

A number of spectra were taken at each temperature with broadening gas pressures up to 1500 Pa. Between three and five broadening measurements were made for each broadening gas and pressure with, typically, four to six separate spectral scans contributing to each measurement.

For H_2, He, and N_2 broadening, a trace amount of NO_2 was added with the broadening gas to produce OH. NO_2 is used in sufficiently small amounts that correction for its broadening is negligible. For the mixtures containing O_2 the NO_2 was not necessary. The concentration of unreacted hydrogen atoms is negligible. H_2 was taken from a gas cylinder at room temperature, and all H_2 used in the broadening studies entered the cell through the dc discharge. No attempt was made to determine changes in the *ortho/para* hydrogen ratio caused by the discharge. For the N_2 and O_2 broadening studies, an amount of He equal to $\sim\frac{1}{2}$ of the total pressure was necessary to obtain sufficient OH signal. Central absorption of the stronger OH line was measured for the various mixtures to ensure that it remained low (usually <5%) to avoid saturation broadening of the lines.

Figure 1a–d shows broadening of the OH lines for a range of pressures by N_2 and He, as well as the fitted spectra used for determinations of pressure broadening coefficients, as discussed below.

DATA ANALYSIS AND RESULTS

Spectra are fitted with a nonlinear least-squares routine to modulation-broadened Voigt derivative line profiles, including the time constant for phase detection used in the measurements. Synthetic spectra are generated with fixed Gaussian cores. Lor-

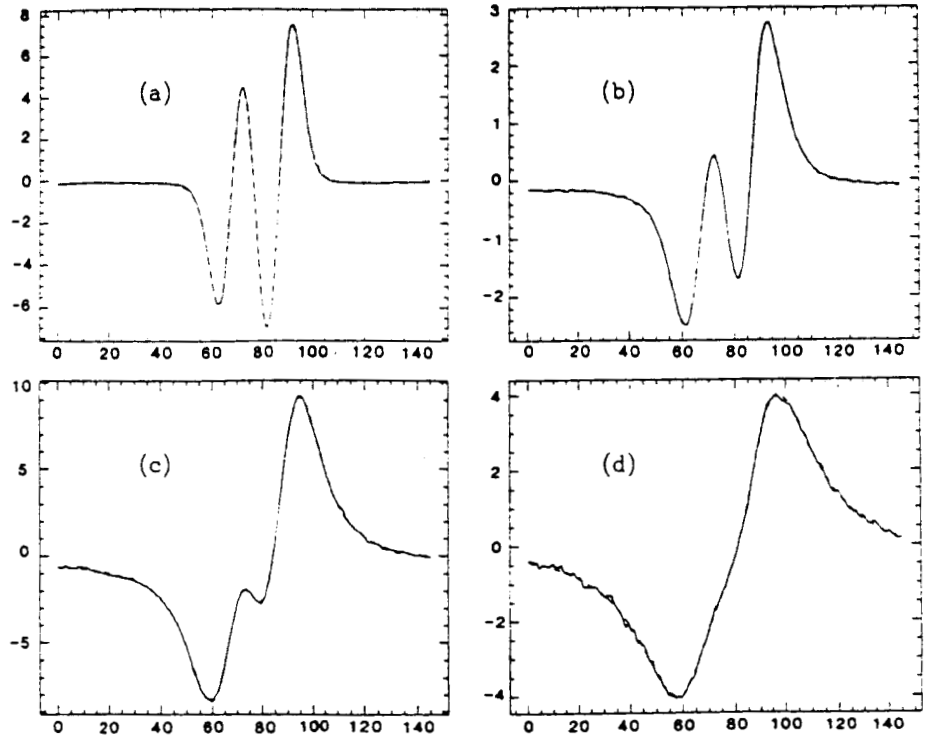

FIG. 1. Absorption measurements of OH broadened by He and N_2. The nonlinear least-squares fits to the spectra are shown as dashed lines. Spectra shown in the figure are for 296 K measurements of broadening by: (a) 143 Pa He; (b) 314 Pa N_2 + He; (c) 642 Pa N_2 + He; (d) 1127 Pa N_2 + He. The scan width, shown in the abscissas, is 145 MHz, from 3 551 272.030 to 3 551 127.030 MHz. The intensity scales are arbitrary.

entzian widths, positions, intensities, and baseline corrections are varied in the fitting. Spectra are corrected for the gain curve of the tunable waveguide laser by using power curve spectral scans taken at regular intervals.

The OH F_1, $7/2^+ \leftarrow F_1$, $5/2^-$ spectrum is split by the hyperfine interaction into three lines. Two of these, the $F = 3 \leftarrow 2$ (on the left) and the $F = 4 \leftarrow 3$ (on the

TABLE I

Pressure Broadening Coefficients (10^{-7} cm^{-1}-Pa^{-1}, HWHM) for the 118.455 cm^{-1} Lines of OH[a]

Broadening gas	Temperature (K) 296	259	210	80
H_2	6.92(21)	7.11(21)	8.55(35)	13.2(1.2)
He	1.75(15)	2.05(06)	2.70(10)	1.85(20)
N_2	9.00(27)	8.89(35)	9.05(27)	-
O_2	4.74(1.21)	5.02(15)	3.63(54)	-
Air[b]	8.10(47)	8.08(31)	7.91(33)	-

[a] 2σ uncertainties shown. One atmosphere = 1.01325×10^5 Pascal (Pa).
[b] $\gamma_{air} = 0.79\gamma_{N_2} + 0.21\gamma_{O_2}$.

right), are visible in the spectral scans shown in Fig. 1 (note that the scans are down in frequency). A third, much weaker line, $F = 3 \leftarrow 3$, lies under the $F = 4 \leftarrow 3$ line, at 0.66 MHz higher frequency (*10*). This line is also included in the fitting, with its frequency, width, and relative strength locked to the $F = 4 \leftarrow 3$ line. The widths for the two large hyperfine components are fitted separately.

The spectrum fitting results for helium broadening measurements are corrected for the hydrogen broadening contribution to the total linewidths. N_2 and O_2 broadening measurements are corrected for H_2 and He contributions. The corrected linewidths and pressures for each gas at each temperature are used in weighted linear regressions to determine the pressure broadening coefficients. The regressions were first performed separately on the fitting results for the two large hyperfine components. No statistically significant differences in broadening of the two components for any of the broadening gases at any of the measurement temperatures were noted. The $F = 4 \leftarrow 3$ and $F = 3 \leftarrow 2$ widths are averaged before the final regression analysis. The resulting pressure broadening coefficients and their 2σ uncertainties are given in Table I. The uncertainties from the fitting procedure include the nonlinear least-squares fitting errors, pressure and flow uncertainties, power curve variations, uncertainties due to line saturation broadening, and the statistical uncertainties from the regression analysis. We have also included air-broadening coefficients in Table I, calculated as $\gamma_{air} = 0.79\gamma_{N_2} + 0.21\gamma_{O_2}$.

We also attempted to determine pressure-induced shifts of the OH lines from the least-squares fitted line positions, using the same regression technique as for the linewidths. It was not possible with the present data set to obtain statistically significant pressure shifting coefficients. It was possible to make a slightly more accurate determination of the positions of the OH lines from the present measurements, from the He-broadened lines at the lowest pressure. Our positions and their 2σ uncertainties are 3 551 185.36(4) MHz ($4 \leftarrow 3$), and 3 551 204.42(4) MHz ($3 \leftarrow 2$).

DISCUSSION

There are no other laboratory measurements of pressure broadening of these lines for direct comparison with our results. There are results from several studies for other OH lines at room temperature. Burrows *et al.* (*18*) have measured broadening by He, Ar, and NO_2 of the F_1, $5/2^+ \leftarrow F_1$, $3/2^-$ and F_1, $5/2^- \leftarrow F_1$, $3/2^+$ lines at 2.528 THz using laser magnetic resonance. Their only point of comparison with our study is for He broadening. Their value of 2.21×10^{-7} cm^{-1}-Pa^{-1} (0.89 MHz-Torr^{-1}; note that they report the FWHM Lorentzian parameters) compares favorably with our value of 1.75×10^{-7} (0.70 MHz-Torr^{-1}), considering that the measurements are of different lines. The difference is in the correct direction for the expected decrease in pressure broadening coefficient with increase in rotational energy. In a microwave study of the Λ-doublet transitions of OH with $J = \frac{7}{2}$ in the 13.4 GHz region, Bastard *et al.* obtain broadening results for nine gases, including the four that we have measured (*20*). Agreement between our measurements is quite poor, especially for He broadening (7.5×10^{-7} cm^{-1}-Pa^{-1} vs our value of 1.75×10^{-7}). Line broadening calculations should be able to resolve whether the large differences arise because of the different transitions involved.

Buffa *et al.* (*20*) have used Anderson theory to calculate the N_2 broadening of several far-infrared lines of OH, including the lines studied here, for a range of temperatures (*21*). Their calculation at 300 K compares quite well with our measurements (they calculate 9.7×10^{-7} cm^{-1}-Pa^{-1} vs our value of 9.0×10^{-7} cm^{-1}-Pa^{-1} at 296 K). Their calculation at 200 K is, however, substantially different than our value at 210 K (1.2×10^{-6} cm^{-1}-Pa^{-1} calculated vs 9.0×10^{-7} cm^{-1}-Pa^{-1} measured). This difference chiefly reflects a departure from the expected temperature dependence for interactions that are primarily dipole–quadrupole. The calculations demonstrate the expected temperature dependence while our measurements, for both N_2 and O_2 broadening, show very little temperature dependence.

ACKNOWLEDGMENTS

The authors thank G. Melnick of the Harvard–Smithsonian Center for Astrophysics and J. M. Brown of Oxford University for helpful discussions. L. R. Zink provided invaluable help with the TuFIR apparatus. The research at the Smithsonian Astrophysical Observatory and the University of Oregon was supported by NASA (NAGW-1292, NAG-1-963). Research at the National Institute for Standards and Technology was partially supported by NASA (W-15, 047).

RECEIVED: November 6, 1990

REFERENCES

1. K. V. CHANCE, W. A. TRAUB, B. CARLI, I. G. NOLT, AND J. V. RADOSTITZ, "Proc. AIAA/NASA Earth Observing System Conference," AIAA-85-3006, 1985.
2. D. J. W. KENDALL AND T. A. CLARK, *J. Quant. Spectrosc. Radiat. Transfer* **21**, 511–526 (1979).
3. D. J. W. KENDALL AND T. A. CLARK, *Nature* **283**, 57–58 (1980).
4. B. CARLI, F. MENCARAGLIA, A. BONETTI, M. CARLOTTI, AND I. NOLT, *Int. J. Infrared Millimeter Waves* **6**, 149–176 (1985).
5. B. CARLI, B. M. DINELLI, F. MENCARAGLIA, AND J. H. PARK, *J. Geophys. Res.* **94**, 11 049–11 058 (1989).
6. W. L. MEERTS AND A. DYMANUS, *Chem. Phys. Lett.* **23**, 45–47 (1973).
7. W. L. MEERTS AND A. DYMANUS, *Canad. J. Phys.* **53**, 2123–2141 (1975).
8. J. FARHOOMAND, G. A. BLAKE, AND H. M. PICKETT, *Astrophys. J.* **291**, L19–L22 (1985).
9. J. M. BROWN, L. R. ZINK, D. A. JENNINGS, K. M. EVENSON, A. HINZ, AND I. G. NOLT, *Astrophys. J.* **307**, 410–413 (1986).
10. D. M. WATSON, R. GENZEL, C. H. TOWNES, AND J. W. V. STOREY, *Astrophys. J.* **298**, 316–327 (1985).
11. G. J. MELNICK, R. GENZEL, AND J. B. LUGTEN, *Astrophys. J.* **231**, 530–542 (1987).
12. G. J. MELNICK, G. J. STACEY, R. GENZEL, J. B. LUGTEN, AND A. POGLITSCH, *Astrophys. J.* **348**, 161–168 (1990).
13. J. H. BLACK AND E. F. VAN DISHOECK, *in* "Masers, Molecules, and Mass Outflows in Star Forming Regions" (A. D. Haschick, Ed.), p. 43, Haystack Observatory, 1985.
14. R. SCHINKE AND P. ANDRESEN, *J. Chem. Phys.* **81**, 5644–5648 (1984).
15. D. P. DEWANGEN AND D. R. FLOWER, *J. Phys. B* **14**, 2179–2190 (1981).
16. K. M. EVENSON, D. A. JENNINGS, AND F. R. PETERSON, *J. Appl. Phys.* **44**, 576–578 (1984).
17. I. G. NOLT, J. V. RADOSTITZ, G. DILONARDO, K. M. EVENSON, D. A. JENNINGS, K. R. LEOPOLD, M. D. VANEK, L. R. ZINK, A. HINZ, AND K. V. CHANCE, *J. Mol. Spectrosc.* **125**, 274–287 (1987).
18. J. P. BURROWS, D. I. CLIFF, P. B. DAVIES, G. W. HARRIS, B. A. THRUSH, AND J. P. T. WILKINSON, *Chem. Phys. Lett.* **65**, 197–200 (1979).
19. D. BASTARD, D. A. BRETENOUX, A. CHARRU, AND F. PICHERIT, *J. Quant. Spectrosc. Radiat. Transfer* **21**, 369–372 (1979).
20. G. BUFFA, O. TARRINI, AND M. INGUSCIO, *Appl. Opt.* **26**, 3066–3068 (1987).